



Preparation and characterization of nickel aluminosilicate nanocomposites for transfer hydrogenation of carbonyl compounds

N. Neelakandeswari^a, G. Sangami^a, P. Emayavaramban^a, S. Ganesh Babu^b,
R. Karvembu^b, N. Dharmaraj^{a,*}

^a Department of Chemistry, Bharathiar University, Coimbatore 641 046, India

^b Department of Chemistry, National Institute of Technology, Tiruchirappalli 620 015, India

ARTICLE INFO

Article history:

Received 1 July 2011

Received in revised form

15 September 2011

Accepted 31 December 2011

Available online 10 January 2012

Keywords:

Nickel aluminosilicate

Carbonyl compounds

Quinoline carboxaldehyde

Transfer hydrogenation

Heterogeneous catalysis

ABSTRACT

Three different samples of nickel aluminosilicate (NAS) nanocomposite for application as catalyst in transfer hydrogenation reactions were prepared by the incorporation of nickel nanoparticles into the mesoporous aluminosilicate framework obtained by a simple sol–gel method followed by calcinations at various temperatures without using any templates. The above prepared nanocomposites were characterized using thermal studies, Fourier transform infrared (FT-IR) spectroscopy, powder X-ray diffraction (XRD) analysis, scanning electron microscopy (SEM), energy dispersive X-ray analysis (EDAX), transmission electron microscopy (TEM), X-ray photoelectron spectroscopy (XPS) and nitrogen adsorption–desorption (BET) analysis. Effect of calcination temperature of aluminosilicate support on the surface area and pore size of the nanocomposites was studied from BET analysis. Crystalline nature and particle size of nickel oxide present in the aluminosilicate framework was determined from powder XRD pattern. Surface morphology of the catalysts and their elemental compositions were obtained from SEM and EDAX techniques, respectively. Catalytic activity of the above prepared catalysts towards transfer hydrogenation (TH) of carbonyl compounds using isopropyl alcohol as hydrogen donor in presence of KOH was tested with wide range of carbonyl compounds. The yield of the products formed in TH reaction was monitored by gas chromatography (GC).

© 2012 Elsevier B.V. All rights reserved.

1. Introduction

Nanostructured materials receive much attention as catalysts by virtue of their unique properties of large surface area and textural characteristics. Though nanomaterials serve as an excellent heterogeneous catalyst, often they need an additional support to acquire thermal stability. Varieties of materials like TiO₂, Al₂O₃, SiO₂, zeolites/aluminosilicates, chitosan, carbon nanotubes, etc., have been used as supports for nanocatalysts [1–6]. Among these materials, aluminosilicates are widely used as catalyst and also support for a number of reactions. Aluminosilicate frameworks are formed by the condensation of tetrahedral aluminate and silicate complexes via their corner units. Net negative charge created on the surface during the incorporation of AlO₄⁵⁻ for SiO₄⁴⁻ leads to the surface acidity of these materials and hence the ion exchange is feasible on the surface [7] and also a decrease in the molar ratio of SiO₂/Al₂O₃ in the framework leads to an increase in the ion-exchange

capacity and hence the maximum loading of transition metal ions [8]. Though there are varieties of methods available for the preparation of aluminosilicates including sol–gel, co-precipitation, substitution, hydrothermal routes, etc., sol–gel technique is one of the frontier methods often used method for the preparation of homogeneous aluminosilicates from organic precursors at considerably low temperature [9].

When a nanosized material is distributed on an amorphous or crystalline matrix of the above mentioned type, nanocomposite materials are obtained. Currently, nanocomposites are considered as interesting materials because of their potential applications based on the improved physical and chemical properties. Incorporation of transition metal nanoparticles/metal oxides on the aluminosilicate is of great interest and possesses the combined effects of high surface area and porosity of the aluminosilicates with the catalytic properties of metal/metal oxide nanoparticles and they can be obtained by simple impregnation process. Over a long period, nickel based catalysts have been studied as the best systems for hydrogenation, dehydrogenation, hydrocyanation and isomerization reactions and are more active at the nanoscale. Nickel incorporated aluminosilicate nanocomposites were also used as a catalyst for the epoxidation of cyclooctane [10]. Selective

* Corresponding author. Tel.: +91 422 2428316; fax: +91 422 2422387.
E-mail address: dharmaraj@buc.edu.in (N. Dharmaraj).

hydrogenation of carbonyl compounds to their corresponding alcohols is an industrially important transformation reaction. Among the methodologies employed for hydrogenation reactions, catalytic transfer hydrogenation reactions under heterogeneous conditions are the widely used pathway both in laboratory and industry owing to the advantages such as mild reaction conditions and the use of non-toxic hydrogen transfer agents like isopropyl alcohol and hydrazine. Nickel nanoparticles have been extensively studied for the transfer hydrogenation of carbonyl compounds and olefins to their corresponding alcohols and alkanes, respectively [11,12]. However, the use of nanoparticles without a support will lead to agglomeration of the active catalyst and also difficulty in separation from the reaction mixture [13,14]. In order to increase the life time of the catalyst, it is necessary to stabilize the nano catalyst from agglomeration and it is expected that the loading of nanoparticles on the aluminosilicate framework will increase the catalytic activity due to the additional porous nature and acidity of the support. In this work, we present the preparation and characterization of mesoporous nickel aluminosilicate nanocomposites through sol–gel method for transfer hydrogenation of a series of aromatic carbonyl compounds and few *N*-heterocyclic aldehydes into their respective alcohols.

2. Experimental

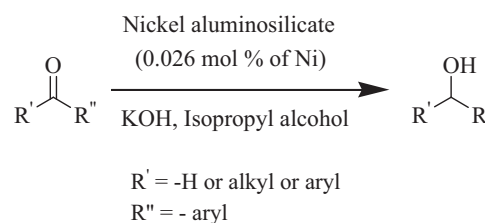
2.1. Preparation of catalyst

All the chemicals used were of reagent and analytical grade. Tetraethyl orthosilicate (TEOS) and aluminium nitrate were purchased from Aldrich and used as received without any further purification. Absolute alcohol, nickel chloride, potassium hydroxide, isopropyl alcohol, ethyl acetate and ammonia were obtained from Merck India Pvt. Ltd. and used as such.

Clear solutions of aluminium nitrate (0.32 M) and TEOS (0.63 M) prepared separately in ethanol in 3:2 ratio were mixed together and the pH of the medium was adjusted to 9 with ammonia and stirred for 24 h at room temperature. The sol obtained was allowed for gelation at room temperature for 5 days. Since the concentration of water affects the rate of hydrolysis and condensation, ratio of water to alcohol was maintained as 1:16. The gel obtained was calcined at 800 °C, 1000 °C and 1200 °C to get the aluminosilicate support and were named as AS-1, AS-2, AS-3, respectively. The above prepared aluminosilicate supports were stirred with 0.1 M aqueous NiCl₂·6H₂O solution for 3 days repeatedly washed with water and dried at room temperature. Finally Ni²⁺ incorporated AS-1, AS-2 and AS-3 was reduced with hydrazine to get the nickel aluminosilicate nanocomposites and were named as NAS-1, NAS-2 and NAS-3, respectively, and used as heterogeneous catalysts for transfer hydrogenation of a series of carbonyl compounds.

2.2. Characterization of catalyst

Thermal analysis and TG-DTA of the samples were recorded with Pyris/Diamond thermal analyser. Infra-red spectra of different samples were recorded as KBr discs with Nicolet Avatar model FT-IR spectrophotometer between 400 and 4000 cm⁻¹. Powder X-ray diffraction patterns of the nanocomposites were obtained using X'PERT Panalytical X-ray diffractometer (Cu-Kα radiation λ = 1.54056 Å) equipped with a scanning rate of 0.02°/s in 2θ range from 10° to 90°. The textural properties of the materials were analyzed by N₂ adsorption/desorption measurements using Micromeritics ASAP 2020 Porosimeter instrument. Pore size distribution was obtained by applying the BJH pore analysis to the adsorption branch of the nitrogen adsorption–desorption isotherms. Scanning electron microscopic (SEM) images were



Scheme 1. Transfer hydrogenation of carbonyl compounds.

recorded on JEOL JSM-6390 instrument equipped with an energy dispersive X-ray analysis (EDAX). TEM analysis of the sample was done with a copper grid dipped in a dispersion in ethanol using JEOL JEM 2100 microscope. Temperature programmed reduction (TPR) was carried out on the preheated samples in a U-shaped quartz reactor with 15% H₂/Ar gas flow of 25 cm³/min. Hydrogen consumption was monitored as a function of temperature with thermal conductivity detector in a Micromeritics autochem II chemisorption instrument. Gas chromatographic analysis of alcohols and carbonyl compounds was done with Shimadzu-2010 gas chromatograph (GC). Nuclear magnetic resonance (NMR) spectra of selected products were recorded with Bruker AMX 500 at 500 MHz with tetramethyl silane as internal standard in DMSO solvent.

2.3. Transfer hydrogenation of carbonyl compounds

A reaction mixture consisting of the respective catalyst NAS1 (30 mg; 0.026 mol% of Ni), substrate (0.5 mmol), isopropyl alcohol (3 mL) and KOH (1.0 mmol) were refluxed at 90 °C for 30 min or 3 h in the case of aldehydes or ketones) as substrates respectively (Scheme 1). Then the catalyst was separated by centrifugation and the centrifugate was washed with water, extracted with ethylacetate and analyzed by GC. Authentic samples of both the substrates and corresponding products were used to verify the retention times and to confirm the formation of products. The used catalyst was washed with isopropyl alcohol and water for several times and used for subsequent transfer hydrogenation reactions in order to test its reusability.

2.4. Product analysis

Gas chromatograph equipped with 5% diphenyl and 95% dimethyl siloxane, Restek capillary column (60 m length, 0.32 mm dia) and a flame ionization detector (FID) was employed to analyze the reaction mixture. Initial column temperature was increased from 60 to 150 °C at a rate of 10 °C/min and then to 220 °C at the rate of 40 °C/min. Nitrogen was used as a carrier gas. The temperatures of the injection port and FID were kept constant at 150 and 250 °C, respectively during the product analysis.

3. Results and discussion

Thermogram of the aluminosilicate gel obtained after 5 days of gelation is given in Fig. 1. The weight losses observed around 80 °C and 120 °C were assigned to the loss of surface bound water molecules and the water molecules formed from the condensation of terminal –OH groups. Decomposition of organic moieties around 280 °C leads to a drastic weight loss in TG along with an endotherm in the DTA. In addition, a very small endotherm appeared around 700 °C in DTA without any corresponding weight loss in TG is attributed to the phase transformation of the amorphous aluminosilicate into the crystalline form. Based on the information derived from TG/DTA, the as-prepared gels were calcined at 800 °C, 1000 °C and 1200 °C to obtain three different samples of aluminosilicates AS1, AS2 and AS3, respectively.

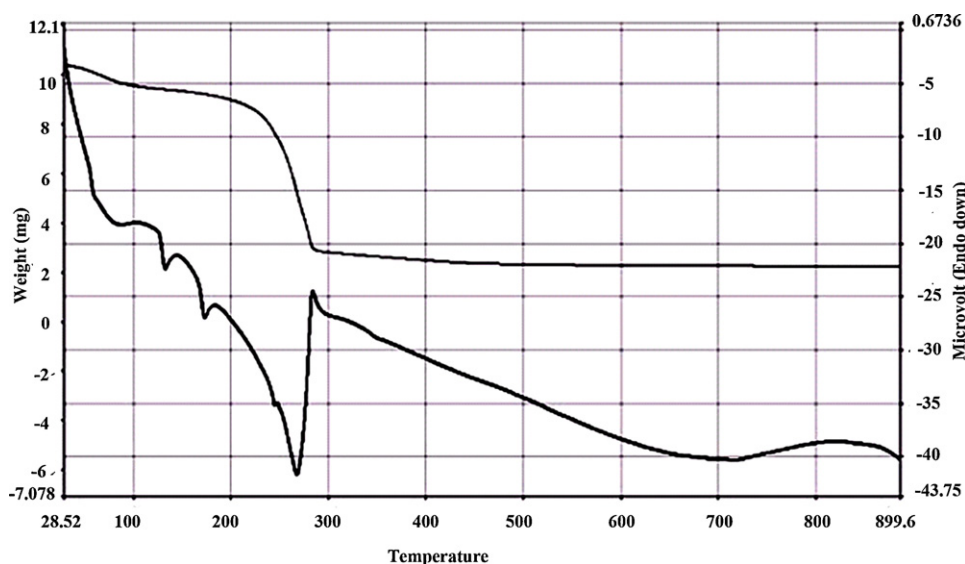


Fig. 1. TGA/DTA of aluminosilicate.

The IR spectra of the aluminosilicate support and respective nickel containing catalysts are given in Fig. 2. The non-existence of any absorption in the $3750\text{--}3745\text{ cm}^{-1}$ region corresponding to the free silanol groups on the surface of the catalyst revealed that all the silanol monomeric units got polymerized during the aging period. In general, stretching frequencies are sensitive to Si/Al composition on the framework and shift to lower frequency with increasing number of tetrahedral aluminium atoms. Strong bands were present in the region $950\text{--}1250\text{ cm}^{-1}$ in the IR spectra of all the supports due to the stretching vibrations of internal tetrahedral units and are the typical vibrations found in all types of zeolites. Bands due to bending vibrations of tetrahedral units were found between 650 cm^{-1} and 800 cm^{-1} [8]. Vibrational bands appeared in the region of $500\text{--}600\text{ cm}^{-1}$ arises due to the linkages between the tetrahedral units. These IR bands observed in the spectra of all the aluminosilicate samples (AS1, AS2 and AS3) calcined at various temperatures confirmed the formation of zeolite like structure. Further the loading of nickel on the zeolite framework did not show any extra bands but a slight decrease in the stretching and bending vibrations of the tetrahedral units and this shed some light on the incorporation of nickel on the tetrahedral sites of the zeolite framework [8].

Powder XRD patterns of the aluminosilicate supports AS1, AS2 and AS3 showed that the crystallinity of the samples increased with the calcination temperature (Fig. 3a). The diffraction patterns of nickel loaded aluminosilicate nanocomposites NAS1, NAS2 and NAS3 displayed all the peaks similar to that of the aluminosilicate support with an additional strong diffraction at $2\theta = 18.3^\circ$ that was assigned to Ni as cubic nickel oxide with face centered lattice by comparison with the standard JCPDS file (JCPDS file No. 89–5881). The nickel nanoparticles formed on the surface of the supports were converted to its oxide that gave the above strong diffraction. The observed patterns of the supports and nickel loaded nanocomposites were indexed to the respective planes in Fig. 3(b). Further, the crystallite size of the nickel oxide nanoparticles calculated using the Scherrer formula was found to be 4.68 nm, 5.24 nm and 5.87 nm in the samples of NAS1, NAS2 and NAS3, respectively. A slight increase in the crystallite size of NiO along (111) plane was observed as a function of calcination temperature of the aluminosilicate support.

Surface morphology and porous nature of the nanocomposite catalysts NAS 1, NAS 2 and NAS 3 were analyzed through scanning electron microscopic images. From the SEM images, the layered porous morphology of the catalysts were identified (Fig. 4). The

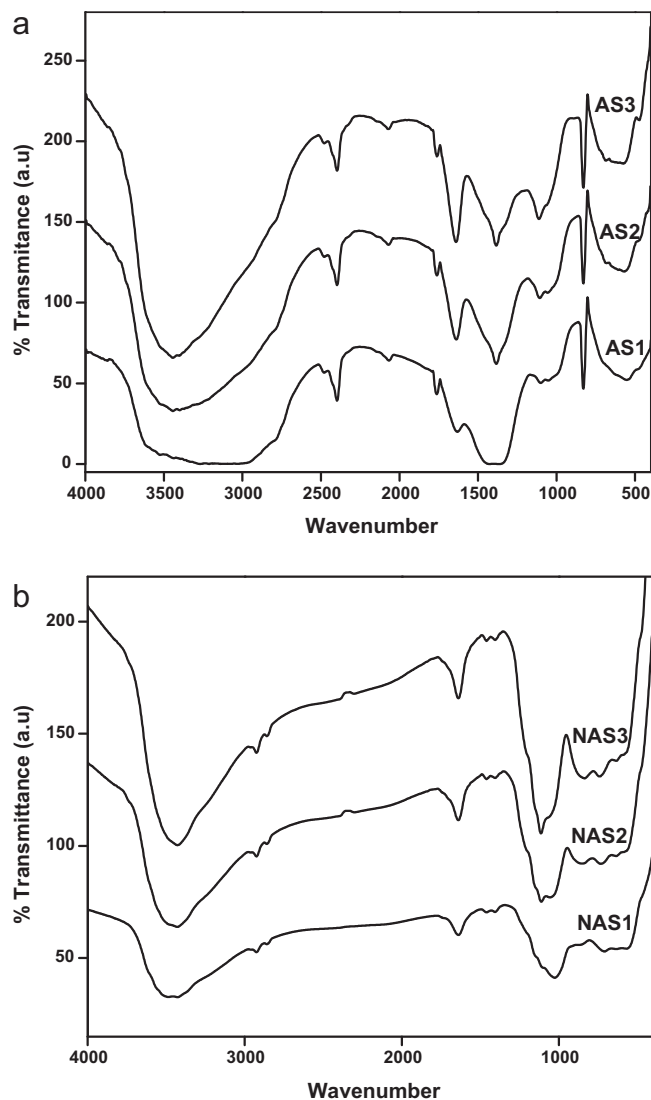


Fig. 2. FT-IR spectra of (a) aluminosilicate support and (b) nickel aluminosilicate catalysts.

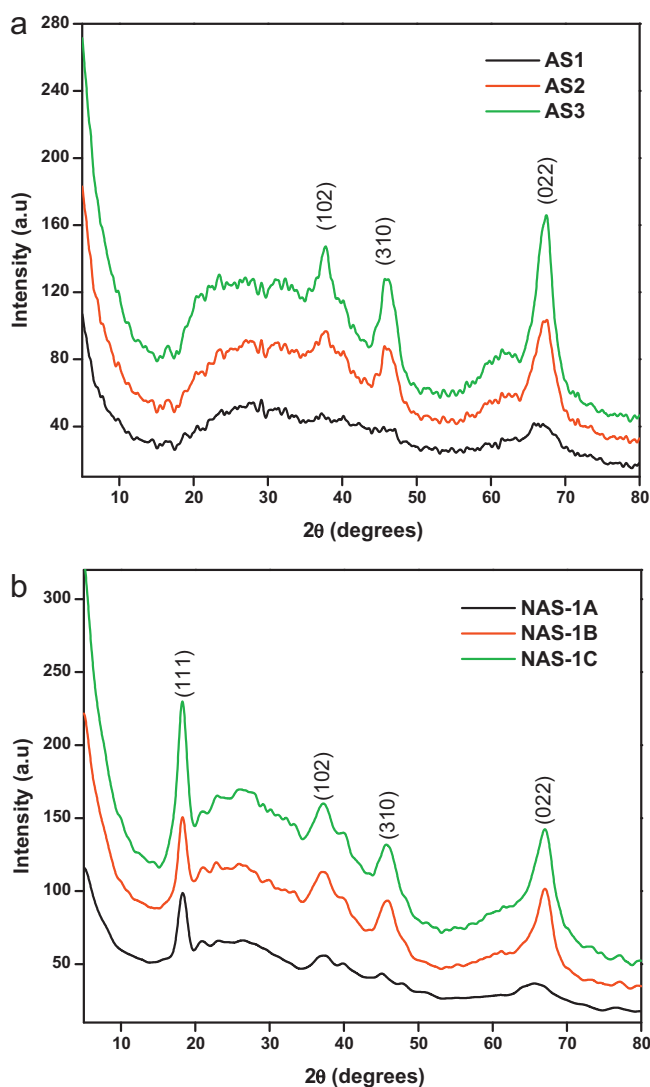


Fig. 3. XRD patterns of (a) support, (b) NAS catalysts calcined at various temperatures.

elemental composition of the catalysts was analyzed using energy dispersive X-ray analysis technique and the results were tabulated (Table 1). The amount of nickel loaded on the aluminosilicates decreased gradually with respect to both the increase in the Si/Al ratio on the surface as well as calcination temperature. In general, the amorphous supports have the maximum ion exchange capacity than the crystalline materials, whereas the crystallinity can be controlled by calcination temperature as evidenced from XRD. Further proof regarding the presence of NiO nanoparticles in the framework of the selected catalyst NAS1 was presented with a transmission electron microscopic image with corresponding SAED pattern and HRTEM image (Fig. 5).

Surface area, pore diameter, pore volume and pore size distribution were calculated using the nitrogen adsorption–desorption isotherm and the results were summarized in Table 2. The BET

Table 1
Elemental composition of NAS.

Sample code	O mass (%)	Al mass (%)	Si mass (%)	Ni mass (%)
NAS 1	65.92	36.53	8.86	0.19
NAS 2	54.19	25.02	9.09	0.18
NAS 3	67.15	19.05	13.63	0.17

Table 2
Adsorption–desorption characteristics of NAS.

Catalyst	BET surface area (m ² g ⁻¹)	BJH pore volume (cm ³ g ⁻¹)	BJH pore radius (nm)
NAS1	184.29	0.2633	2.9
NAS2	79.88	0.2138	3.4
NAS3	12.35	0.0329	4.6

isotherms (Fig. 6) of the samples NAS1, NAS2 and NAS3 were found to be of type-IV in nature and confirmed the mesoporous nature of these catalyst [15]. Nickel aluminosilicate nanocomposites obtained from the aluminosilicate support calcined at 1000 °C and 1200 °C have experienced a decrease in surface area and porosity in comparison with that of the catalyst obtained using the support calcined at 800 °C and these effects may be attributed to the sintering at high temperatures. This result is in accordance with the increase in crystallinity of the support with calcinations temperature as observed from the XRD data. Further, the broad distribution of the pore size obtained (Fig. 6d–f) is attributed to the disordered pores formed during the capillary evaporation of the solvent in the absence of any external templates.

TPR profile of the catalyst NAS1 is given in Fig. 7 and it contains two successive reductions at 234 °C and 546 °C, respectively. The low temperature reduction consumes only 0.035 mM/g of hydrogen whereas 0.508 mM/g of hydrogen was consumed for the later. This clearly indicates that the major portion of the metallic nickel nanoparticles obtained by reduction with hydrazine is present on the surface of the framework and oxidized to NiO in the atmosphere, whereas a small amount of nickel incorporated inside the mesoporous frame work is stable towards atmospheric oxidation and gave a low temperature desorption peak in the TPR profile [16].

Oxidation state of Ni in the nickel aluminosilicate composite was identified from the XPS spectra. Fig. 8 depicts the XPS spectra of C1s, Ni 2p and survey plot of NAS 1. Ni2p_{3/2} peak appeared at 855.75 eV and 873.35 eV with their corresponding shake up peaks at 861.95 eV and 879.85 eV, respectively. Binding energies of these peaks are assigned to the oxidized form of nickel [17]. Further, the 2p binding energy values of NiO obtained in the present case (855.75 eV) is greater than that of the free NiO (853.5 eV) indicating a strong interaction with the support leading to an enhanced binding energy of the former sample [18]. Existence of these peaks in the spectrum of NAS1 confirmed the atmospheric oxidation of Ni nanoparticles to NiO on its surface. Since XPS is purely a surface technique, the nickel nanoparticles incorporated inside the pores could not be identified from XPS as detected by TPR studies.

3.1. Catalytic transfer hydrogenation reactions

Transfer hydrogenation of carbonyl compounds as a function of catalyst concentration was studied and given in Table 3 by choosing acetophenone as a model substrate with NAS1 catalyst. No conversion of the carbonyl compound into the corresponding alcohol occurred while 10 mg of the NAS1 catalyst was used. However, the catalytic reaction proceeded well with 20 mg of the same catalyst and yielded 81.9% of the reduced product and even it showed further increase to 94% yield with 30 mg of the catalyst. But, further

Table 3
Effect of catalyst quantity on the transfer hydrogenation of acetophenone.

S. no.	Catalyst quantity (mg)	Substrate	Yield (%)
1	10	Acetophenone	0
2	20	Acetophenone	81.9
3	30	Acetophenone	94.0
4	40	Acetophenone	93.6

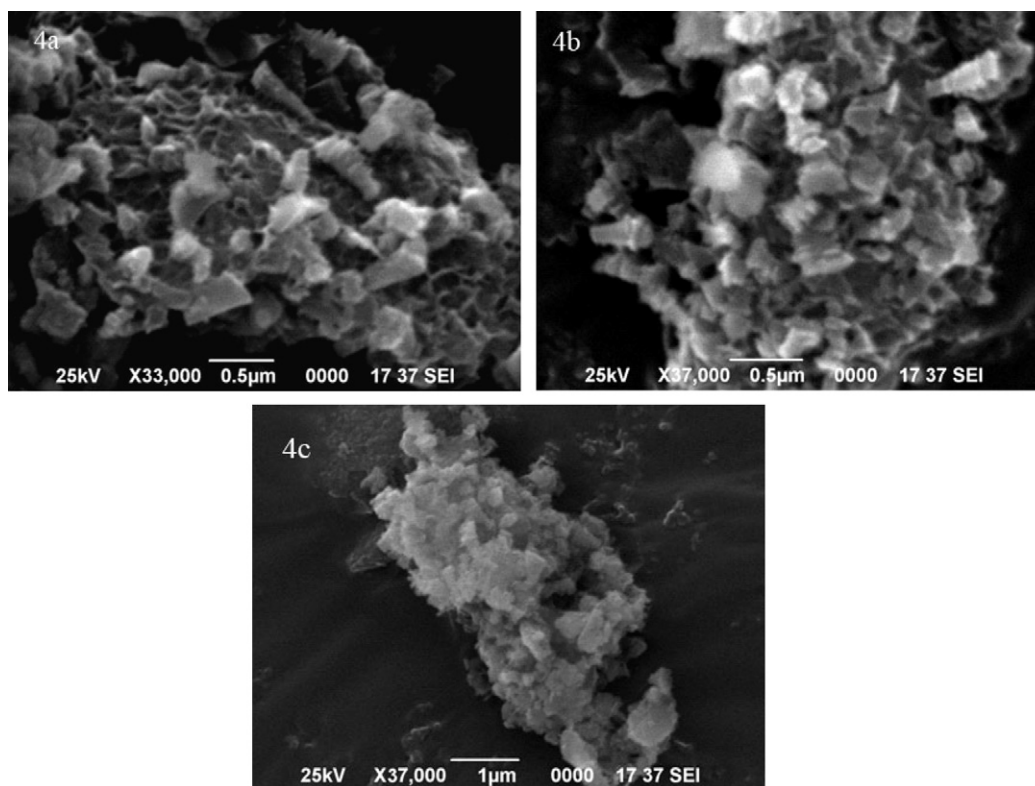


Fig. 4. SEM images of (a) NAS1, (b) NAS2 and (c) NAS3.

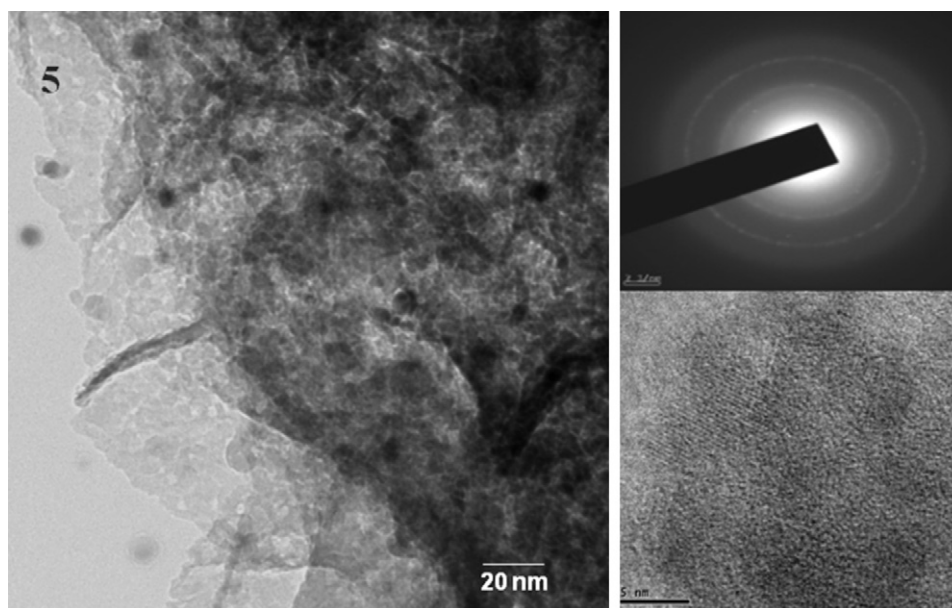


Fig. 5. TEM image of NAS1 with corresponding SAED pattern and HRTEM image.

increase in the catalyst quantity has no remarkable effect on the percentage yield of the product in the transfer hydrogenation reaction and hence the amount of the catalyst was optimized to be 30 mg for all other reactions. When the same reactions were carried out with catalysts NAS2 and NAS3, yield and selectivity of the products were found to be lower than that obtained using NAS1 (Table 4). Decrease in the catalytic efficiency of the samples calcined at different temperature is correlated to the surface area, pore size and ratio of Si/Al on the surface of the catalyst. Compared to NAS1, the surface area and pore size of catalysts NAS2 and NAS3 were

Table 4
Effect of calcination temperature of the aluminosilicate framework on the transfer hydrogenation of acetophenone.

S. no.	Catalyst	Calcination temperature of support (°C)	Substrate	Yield (%)	Selectivity (%)
1	NAS1	800	Benzophenone	99.6	99.6
2	NAS2	1000	Benzophenone	99.4	99.5
3	NAS3	1200	Benzophenone	95.7	98.5

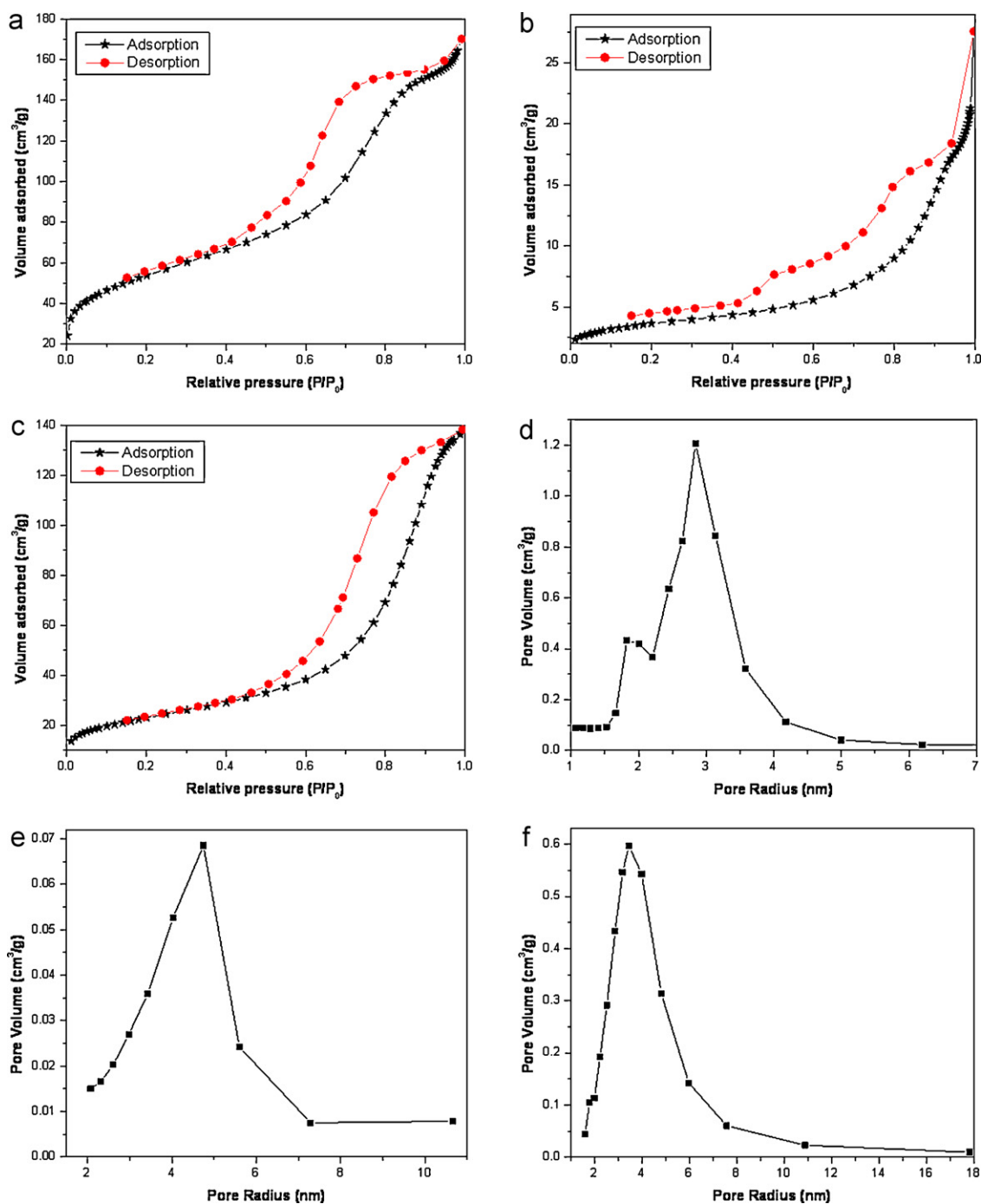


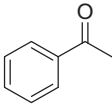
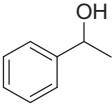
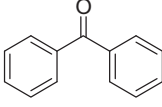
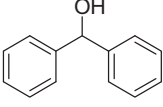
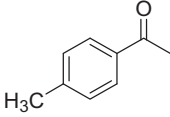
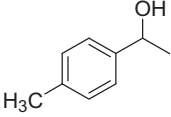
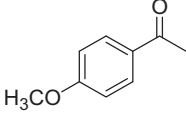
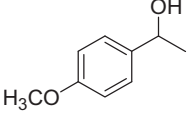
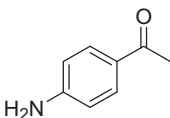
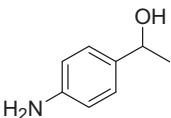
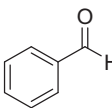
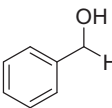
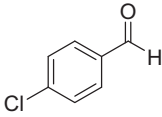
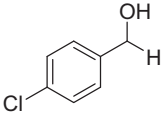
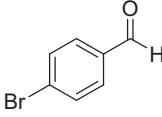
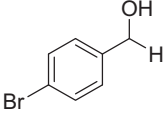
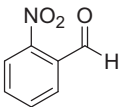
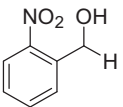
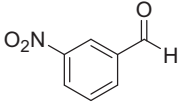
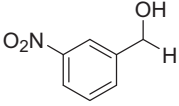
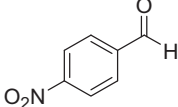
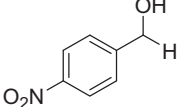
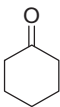
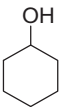
Fig. 6. N_2 adsorption–desorption isotherms of (a) NAS1, (b) NAS2 and (c) NAS3 with corresponding BJH pore size distribution curves of (d) NAS1, (e) NAS2 and (f) NAS3.

very low with high Si/Al ratio on the surface. Low surface area and porosity controls the efficiency of these catalysts towards transfer hydrogenation whereas the ratio of Si/Al on the surface controls the selectivity of them in these reactions. Hence NAS1 was found to be the better catalyst for transfer hydrogenation of carbonyl compounds and the scope was extended to a number of aldehydes and ketones (Table 5). Among the carbonyl groups, aldehydes such as benzaldehyde and its derivatives underwent transfer hydrogenation at a faster rate to yield corresponding alcohols within 30 min of reaction time. (Table 5, entries 6–11; Table 6, entries 4–7) whereas ketones required 3 h as reaction time (Table 5, entries 1–5 and 12; Table 6, entries 1–3). The higher activity of the catalyst towards the transfer hydrogenation of aldehydes can be attributed to the fact

that the carbonyl group of an aldehyde is more electrophilic than ketones and less sterically hindered.

Chemoselectivity of the catalyst NAS1 was further confirmed by the selective reduction of carbonyl group in the presence of halogens, nitro, methoxy, methyl, amino groups, etc., Transfer hydrogenation of *p*-chloro and *p*-bromo benzaldehyde (Table 5, entries 7 and 8) yielded 97.7% and 98.2% of corresponding alcohols, respectively, without affecting the C–X bond with a selectivity of 99.1% and 98.0%. Since heterogeneous catalytic reactions proceed via a six-membered cyclic transition state, rate of such reactions purely depends on the polarizability of carbonyl group on the coordinatively unsaturated site of the catalyst [13]. Though the presence of methyl or methoxy or amino substitution at the para-position of

Table 5
Transfer hydrogenation of carbonyl compounds.

S. no.	Substrate	Product	Reaction time (h)	Yield ^a (%)	Selectivity ^b
1			3.0	94.0	100
2			3.0	99.6 (90.5)	100
3			3.0	70.7	100
4			3.0	71.4	100
5			3.0	99.3	100
6			0.5	85.0	100
7			0.5	98.2 (93.0)	99.1
8			0.5	97.7 (91.0)	98.0
9			0.5	13.1	86.1
10			0.5	88.2	97.7
11			0.5	40.5	44.1
12			0.5	58.4	–

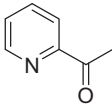
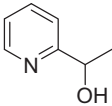
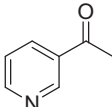
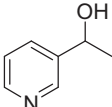
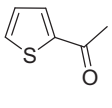
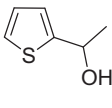
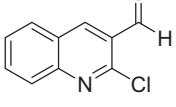
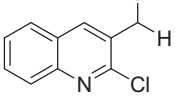
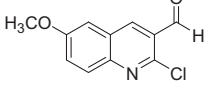
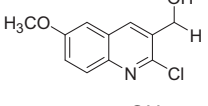
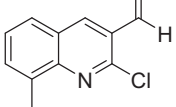
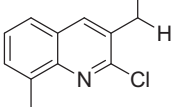
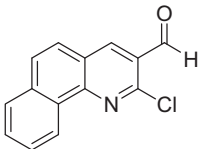
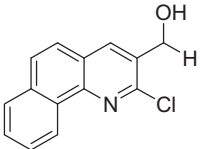
Selectivity = [(area of substrate + area of product)/total peak area] × 100.

Isolated yield in parenthesis.

^a Determined from GC.

^b Determined from GC peak area.

Table 6
Transfer hydrogenation of heterocyclic carbonyl compounds.

S. no.	Substrate	Product	Reaction time (h)	Yield (%)
1			3.0	46.5 ^a
2			3.0	95.7 ^a
3			3.0	48.2 ^a
4			0.5	82.5 ^b
5			0.5	82.3 ^b
6			0.5	82.5 ^b
7			0.5	83.7 ^b

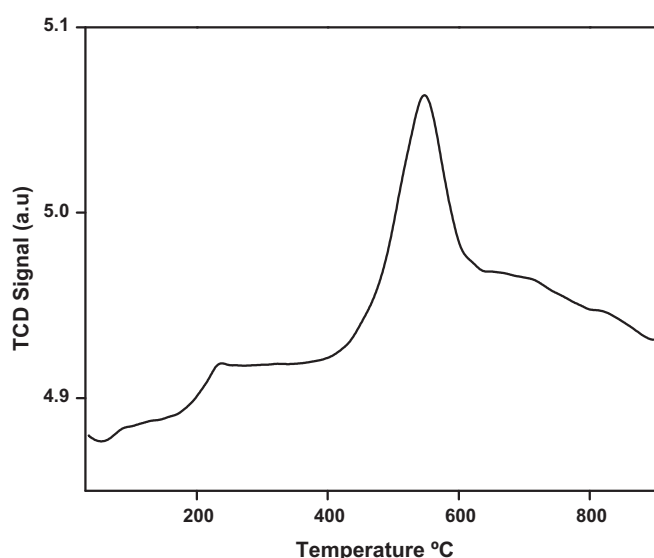
^a GC yield.^b Isolated yield.

Fig. 7. TPR profile of NAS1.

acetophenone was expected to produce almost identical quantity of the respective alcohols (Table 5; entries 3–5), *p*-amino acetophenone afforded significantly higher yield than that of the other two substrates owing to the fact that the more basic amino group present in it could have established a strong interaction with transition metal nickel available in the catalyst leading to an electron deficiency and reduced polarizability of the carbonyl group of the substrate to favour the reduction and formation of more amount of the alcohol. However, the yield of the alcohol obtained (71.4%) during the transfer hydrogenation of 4-methoxy acetophenone in our study using NAS1 within 3 h is significant while compared with that of the same substrate using Ru nanoclusters supported on beta zeolite to yield 92% alcohol after 36 h of reaction time [19].

Heterocyclic carbonyl compounds such as acetylpyridine, acetylthiophene, 2-chloro-3-formylquinoline and its derivatives were also reduced to the corresponding alcohols (Table 6) using the titled catalyst. In this case the transfer hydrogenation of 2-acetylpyridine as well as 2-acetyl thiophene showed a very low alcohol formation in comparison with that of 3-acetylpyridine under identical experimental conditions. 2-Acetylpyridine afforded only 46.5% of respective alcohol while the yield was 95.7% in the case of 3-acetylpyridine and this may be due to the steric effect between the nitrogen atom and the carbonyl group in the 2-acetyl derivative. Similarly, 2-acetyl thiophene also yielded lower product (48.2%). Further, the effect of nitro substitution at

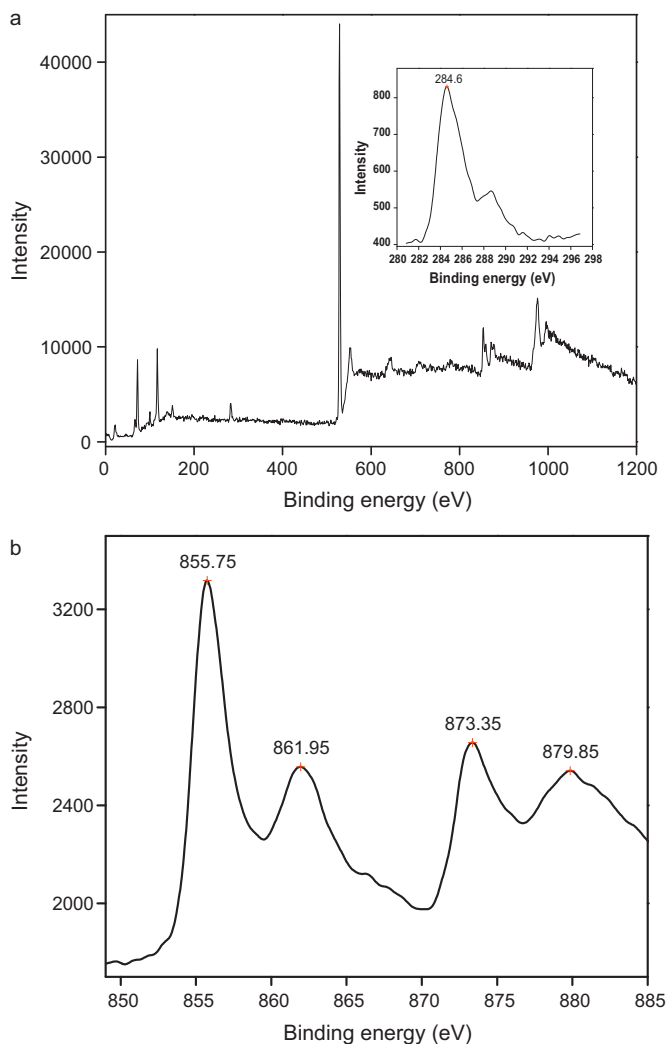


Fig. 8. XPS plot of NAS1 (a) survey with C 1S plot as inset, (b) XPS plot of Ni 2p.

o, *m* and *p*-positions of nitro benzaldehyde was also significant. Among the three positional isomers, *meta* substituted nitro benzaldehyde underwent successful conversion to the corresponding alcohol with 88.2% yield, whereas the *ortho* benzaldehyde gave only 13.0% of the respective alcohol. This behaviour of *ortho* substituted nitro benzaldehyde is very similar to that of the same observed in the case of heterocyclic carbonyl compounds bearing substitution at *ortho* position. Transfer hydrogenation of cyclohexanone yielded only 58.4% of cyclohexanol, which is less than that of majority of the aromatic carbonyl compounds.

2-Chloro 3-formyl quinoline and its derivatives were reduced to their corresponding alcohols and the yields were given in Table 6 (entries 4–7). To our knowledge, there were no much reports on the application of heterogeneous catalysts for the transfer hydrogenation of formyl quinoline and its derivatives. Hence we were interested to undertake the transfer hydrogenation of those biologically important substrates using the above said catalyst NAS1. The products were isolated as mentioned above and their structures were confirmed from the FT-IR and NMR spectral techniques. While comparing the conversion of these carbonyl compounds to their alcohols with that of the reports made using NaBH_4 in presence of a catalyst (montmorillonite K-10) [20,21], our catalytic transfer hydrogenation using isopropyl alcohol yielded >85% isolated alcohol is an efficient and industrially acceptable method. Further, a similar transfer hydrogenation of acetophenone carried

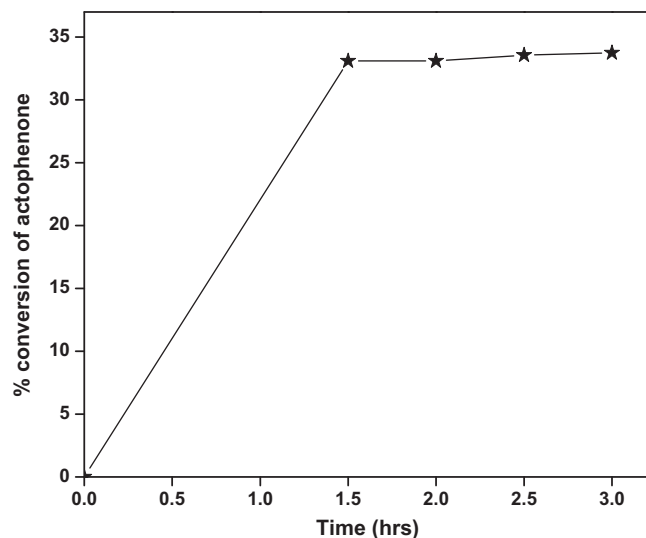


Fig. 9. Heterogeneity test for transfer hydrogenation of acetophenone.

out using commercial NiO nanoparticles without aluminosilicate support yielded only 45% phenylethanol, thereby revealing the significance of support in heterogeneous catalysis.

3.2. ^1H NMR and IR spectral data of various alcohols

3.2.1. (2-Chloro-quinolin-3-yl)-methanol (Table 6, entry 4)

^1H NMR (DMSO): δ = 2.95 (s, 1H, OH), 4.70 (s, 2H, C3- CH_2), 7.66 (t, 1H, J = 7.5 Hz, C6-H), 7.79 (t, 1H, J = 8 Hz, C7-H), 7.97 (d, 1H, J = 8 Hz, C5-H), 8.09 (d, 1H, J = 8 Hz, C8-H) and 8.47 (s, 1H, C4-H).

IR (KBR): ν = 3358 cm^{-1} and 1647 cm^{-1} , respectively, for OH and C=N, respectively.

3.2.2. (2-Chloro-6-methoxy-quinolin-3-yl)-methanol (Table 6, entry 5)

^1H NMR (DMSO): δ = 1.96 (s, 1H, OH), 3.91 (s, 3H, C6- OCH_3), 4.67 (s, 2H, C3- CH_2), 7.41 (dd, 1H, J = 9 Hz, C5-H), 7.50 (d, 1H, J = 3 Hz, C7-H), 7.85 (d, 1H, J = 9 Hz, C8-H), 8.36 (s, 1H, C4-H).

IR (KBR): ν = 3390 cm^{-1} and 1649 cm^{-1} , respectively, for OH and C=N, respectively.

3.2.3. (2-Chloro-8-methyl-quinolin-3-yl)-methanol (Table 6, entry 6)

^1H NMR (DMSO): δ = 1.96 (s, 1H, OH), 2.67 (s, 3H, C8- CH_3), 4.70 (s, 2H, C3- CH_2), 7.53 (t, 1H, J = 8 Hz, C6-H), 7.64 (t, 1H, J = 6 Hz, C7-H), 7.92 (d, 1H, J = 8 Hz, C5-H), 8.44 (s, 1H, C4-H).

IR (KBR): ν = 3390 cm^{-1} and 1644 cm^{-1} , respectively, for OH and C=N, respectively.

3.2.4. (2-Chloro-benzo[h]quinolin-3-yl)-methanol (Table 6, entry 7)

^1H NMR (DMSO): δ = 1.96 (s, 1H, OH), 4.76 (s, 2H, C3- CH_2), 7.78 (m, 2H, C8-H and C9-H), 8.00 (s, 1H, C5-H), 8.07 (m, 1H, C6-H), 8.55 (s, 1H, C4-H), 9.01 (m, 2H, C7-H and C10-H).

IR (KBR): ν = 3386 cm^{-1} and 1590 cm^{-1} , respectively, for OH and C=N, respectively.

3.3. Heterogeneity

Heterogeneous nature of the catalyst was tested by filtering the catalyst after 1.5 h of reaction time, the filtrate was allowed to reflux and was monitored every 30 min for another 1.5 h using GC and the results are given in Fig. 9. Further conversion of acetophenone

Table 7
Reusability of NAS.

S. no.	Recycle	Substrate	GC yield (%)
1	Cycle 1	Acetophenone	94.0
2	Cycle 2	Acetophenone	92.6
3	Cycle 3	Acetophenone	91.9
4	Cycle 4	Acetophenone	91.7

to phenylethanol was not observed even after 3 h. These results proved that the catalytic reactions took place only on the catalyst substrate interface and the nanoparticle was not leached out from the support.

3.4. Reusability

Reusability of heterogeneous catalysts is an important advantage that makes them suitable for industrial applications. The recycling activity of the catalyst NAS1 towards TH reaction was tested with acetophenone as substrate for four cycles and the results were presented in Table 7. The yield of phenyl ethanol obtained after the first run was 94% and no significant loss in catalytic activity was noted upto four cycles that gave 92.57%, 91.91% and 91.68% yield, respectively, after second, third and fourth cycles.

4. Conclusion

Mesoporous nickel aluminosilicate nanocomposites were prepared by a simple sol–gel technique followed by calcination without using any external template. The prepared catalysts were characterized by various physico–chemical techniques. Among the three catalysts prepared NAS1 was found to be an efficient one for the chemoselective, heterogeneous transfer hydrogenation of carbonyl compounds using isopropyl alcohol as hydrogen source. Effect of substituents on the transfer hydrogenation ability was also studied using different substrates. Importantly, the catalyst utilized in our experiments displayed moderate to excellent activity towards the transfer hydrogenation of biologically important formyl quinoline derivatives. The reusability experiment demonstrated that the nickel aluminosilicate catalyst retained its activity up to four cycles. Molecular structure of the products formed by the reduction of some of the heterocyclic aldehydes into corresponding alcohols revealed that the prepared catalyst is selective towards carbonyl group without affecting other functional groups present in the substrate.

Acknowledgement

The authors wish to thank the Department of Science and Technology (DST), New Delhi for the financial support in the form of a major research project (DST File No: SR/SI/IC-45/2007 dated 02.04.08).

Appendix A. Supplementary data

Supplementary data associated with this article can be found, in the online version, at doi:10.1016/j.molcata.2011.12.029.

References

- [1] V. Rodriguez-Gonzalez, S.O. Alfaro, A.A. Zaldivar-Cadena, S.W. Lee, *Catal. Today* 166 (2011) 166–171.
- [2] J. Sun, X. Bao, *Chem. Eur. J.* 14 (2008) 7478–7488.
- [3] R.J. White, R. Luque, V.L. Budarin, J.H. Clark, D.J. Macquarrie, *Chem. Soc. Rev.* 38 (2009) 481–494.
- [4] J.M. Campelo, D. Luna, R. Luque, J.M. Marinias, A.A. Romero, *ChemSusChem* 2 (2009) 18–45.
- [5] L. De'Rogatis, M. Cargnello, V. Gombac, B. Lorenzut, T. Montini, P. Fornasiero, *ChemSusChem* 3 (2010) 24–42.
- [6] H. Sakurai, A. Murugadoss, *J. Mol. Catal. A: Chem.* 341 (2011) 1–6.
- [7] C.F. Chang, Y.L. Wu, S.S. Hou, *Colloids Surf. A* 336 (2009) 159–166.
- [8] B. Viswanathan, S. Sivasanker, A.V. Ramasamy, *Catalysis Principles and Applications*, Narosa Publishing House, New Delhi, 2002.
- [9] P. Padmaja, K.G.K. Warriar, M. Padmanabhan, W. Wunderlich, F.J. Berry, M. Mortimer, N.J. Creamer, *Mater. Chem. Phys.* 95 (2006) 56–61.
- [10] K.J. Ciuffi, E.J. Nassar, L.A. Rocha, Z.N. da Rocha, S. Nakagaki, G. Mata, R. Trujillano, M.A. Vicente, S.A. Korili, A. Gil, *Appl. Catal. A: Gen.* 319 (2007) 153–162.
- [11] F. Alonso, P. Riente, M. Yus, *Acc. Chem. Res.* 44 (2011) 379–391.
- [12] A. Dhakshinamoorthy, K. Pitchumani, *Tetrahedron Lett.* 49 (2008) 1818–1823.
- [13] F. Alonso, P. Riente, J.A. Sirvent, M. Yus, *Appl. Catal. A: Gen.* 378 (2010) 42–51.
- [14] F. Alonso, P. Riente, M. Yus, *Tetrahedron* 65 (2009) 10637–10643.
- [15] S. Brunauer, L.S. Deming, W.E. Deming, E. Teller, *J. Am. Chem. Soc.* 62 (1940) 1723–1732.
- [16] A. Lewandowska, S. Monteverdi, M. Bettahar, M. Ziolek, *J. Mol. Catal. A: Chem.* 188 (2002) 85–95.
- [17] Y. Kolytyn, A. Fernandez, T.C. Rojas, J. Campora, P. Palma, R. Prozorov, A. Gedanken, *Chem. Mater.* 11 (1999) 1331–1335.
- [18] J. Santamaria-Gonzalez, M. Martinez-Lara, A. Jimenez-Lopez, *J. Chem. Soc. Faraday Trans.* 93 (1997) 493–497.
- [19] M.L. Kantam, B.P.C. Rao, B.M. Choudary, B. Sreedhar, *Adv. Synth. Catal.* 348 (2006) 1970–1976.
- [20] M. Akkurt, S.M. Roopan, F.N. Khan, A.S. Kumar, V.R. Hathwar, *Acta Crystallogr. E* 66 (2010), O1542–U1311.
- [21] M.K. Rauf, F.N. Khan, S.M. Roopan, V.R. Hathwar, R. Rajesh, *Acta Crystallogr. E* 66 (2010) O953–O3329.